ELSEVIER

Solar Energy Materials & Solar Cells 69 (2001) 123–129

Solar Energy Materials & Solar Cells

www.elsevier.com/locate/solmat

Dark I–V–T measurements and characteristics of (n) a-Si/(p) c-Si heterojunction solar cells

R. Hussein*, D. Borchert, G. Grabosch, W.R. Fahrner

Chair of Electronic Devices, University of Hagen, P.O. Box 940, D-58084 Hagen, Germany

Abstract

Heterojunction solar cells have been manufactured by depositing n-type a-Si:H on p-type 1–2 Ω cm Cz single-crystalline silicon substrates. An efficiency of 14.2% has been obtained for 1 cm^2 solar cells by using a simple (Al/(p) c-Si/(n) a-Si:H/ITO/metal grid) structure. With an additional surface texturing, we have reached an efficiency of 15.3% for 1 cm^2 solar cells. We have investigated the dark *IV*-curves in order to contribute to a better understanding of the basis of solar cells.

Keywords: Heterojunction; Two-diode model; Dark current

1. Introduction

Earlier the carrier transport in (p) a-Si:H/(n) c-Si heterojunction solar cells in darkness and under varying temperatures was studied. By examining the derivative of the forward dark *IV*-characteristics as a function of voltage and temperature, two separate carrier transport mechanisms are identified at room temperature. At low forward bias voltage and at low-temperatures recombination dominates probably via states in the c-Si depletion region whereas a tunneling mechanism dominates at high temperatures [1].

We investigated the forward dark *IV*-characteristics of (n) a-Si:H/(p) c-Si heterojunction solar cells [2]. At room temperature the *IV*-curves show the typical behavior of the two-diode model.

* Corresponding author. Tel.: + 49-2331-987-2200, fax: + 49-2331-987-321..
E-mail address: reza.hussein@fernuni-hagen.de (R. Hussein).

PII: S0927-0248(00)00385-8

2. . Two-diode model

Fig. 1 shows the equivalent circuit for the two-diode model of a solar cell. The current equation according to the model is as follows:

$$I(V) = I_{D1} + I_{D2} + I_{Rp} + I_L, \tag{1}$$

$$I(V) = I_{01}\left[\exp\frac{q(V-IR_S)}{n_1kT} - 1\right] + I_{02}\left[\exp\frac{q(V-IR_S)}{n_2kT} - 1\right] + \frac{V-IR_S}{R_{sh}} + I_L, \tag{2}$$

where I_{01}, I_{02} are the diode saturation currents, n_1, n_2 are the ideality factors, q is the electron charge, k is Boltzmann's constant, T is the temperature, R_s is the series resistance and R_{sh} is the shunt resistance.

The first two terms of Eq. (2) describe the influences of the diodes. The different current transport mechanisms are expressed by the ideality factors and the saturation currents. The first diode with $n_1 = 1$ expresses the diffusion process within the solar cell at room temperature. With the second diode the different recombination mechanisms are considered, where the theoretically calculated ideality factor comes to $n_2 = 2$. In practice, there is a deviation from this value. Fig. 2 presents the measured dark *IV*-curve at 300 K of a 1 cm^2 solar cell using a semi-logarithmic I–V plot.

From the dark *IV*-curve, we can recognize four different voltage regions (Fig. 2): first region $V < 0.15$ V: the dark current is mainly determined by the shunt resistance R_{sh}. Second region from 0.15 to 0.45 V: the dark current is controlled by the second term of Eq. (2). Third region from 0.45 to 0.6 V: the first term of Eq. (2) dominates. Fourth region from 0.6 V upwards: the dark current is controlled by the series resistance.

The parameters of the model are determined from the analysis of the measured dark *IV*-curve. Subsequently, by inserting the parameters into Eq. (2) the dark *IV*-curve can be calculated numerically.

3. Extraction of model parameters

The shunt and the series resistance can be determined directly from the *IV*-measurement data. In order to extract the diode parameters we have used a semi-logarithmic I–V plot.

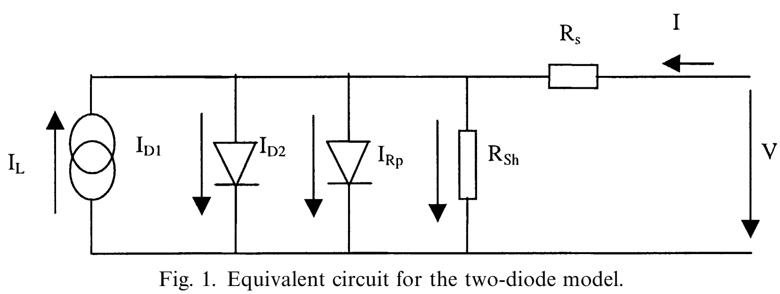

Fig. 1. Equivalent circuit for the two-diode model.

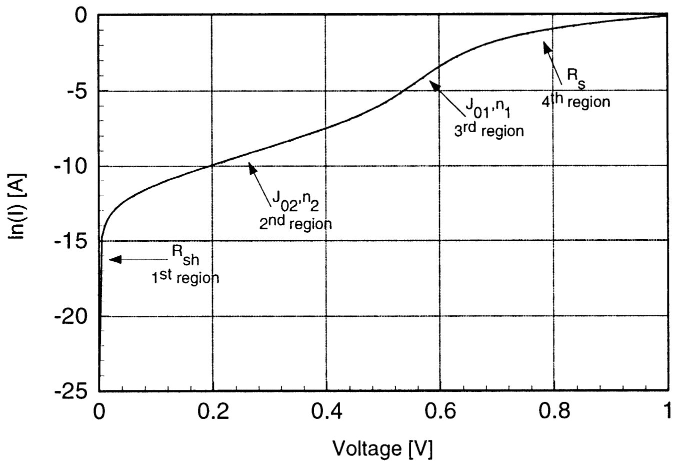

Fig. 2. Dart *IV*-curve with the different regions.

According to Eq. (2), for $I \gg I_0$, we can approximate the two exponential terms in brackets by

$$I_{Di} = I_{0i}\left[\exp\frac{q(V - IR_s)}{n_i kT}\right], \tag{3}$$

$$\ln I_{Di} = \ln I_{0i} + K_i \cdot V' \tag{4}$$

with $i = 1, 2$; $K_i = q/(n_i kT)$ and $V' = V - IR_s$.

By plotting $\ln I_{Di}$ versus V', we get a straight line. The ideality factor n_i can be obtained from the gradient of this line and the intersection on the y-axis delivers the corresponding saturation current I_{0i}

The six parameters determined from the measured *IV*-curve are inserted in Eq. (2) and the equation is numerically solved.

4. Results and discussion

The following parameters can be determined from the measuring curve at room temperature (300 K):

n_1	I_{01} (A)	n_2	I_{02} (A)	R_s (Ω)	R_{sh} (kΩ)
1.03	9.3E-12	3.13	4E-6	0.38	25

The ideality factor $n_1 = 1.03$ coincides with the theoretically assumed value ($n_1 = 1$), i.e., a normal diffusion process takes place. However, there has been a great deviation concerning the ideality factor $n_2 = 3.13$. Considering the generation–recombination

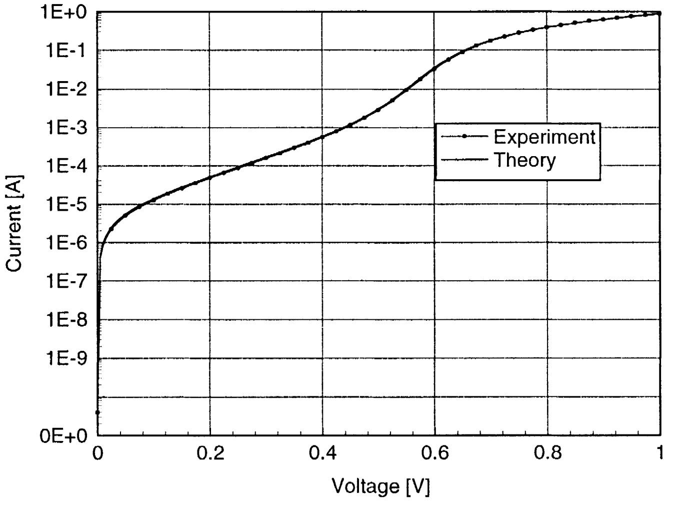

Fig. 3. Comparision of experimental and theoretical dark *IV*-curves at 300 K with the two-diode model.

processes in the depletion region, $n_2 = 2$ has been derived theoretically. Trap states which have been presumed exactly in the middle of the band gap, do not appear there in reality. Moreover, the interface and the surface recombination have not been taken into consideration in the derivation. These simplifications are the main causes for the deviation.

The parameters mentioned above have been inserted in Eq. (2) and the equation has been solved numerically by inputting a voltage area. Fig. 3 shows the comparison between the calculated and the measurement curves and the coincidence of the two curves is very good.

Additionally, it is important to check the validity of the superposition principle: illuminated *IV*-curve = dark *IV*-curve + photocurrent. The investigated solar cells show no voltage dependence of the photocurrent. Table 1 compares the calculated and measured solar cell parameters at 300 K. It can be seen that the coincidence is very good. This is a further proof of the voltage independence of the photocurrent. Table 1 compared the measured and calculated solar cell [2] parameters at 300 K. For the calculations the dark *IV*-curves and the short-circuit currents were used.

In order to determine the temperature dependence of the parameters, especially of the ideality factors, the dark *IV*-curves have been measured at various temperatures. Fig. 4 shows the measurement curves in the range of 300–100 K in 20 K steps.

We can see that the third region shifts towards higher voltages with decreasing temperature from 300 K down to 200 K. The parameters are determined according to the two-diode model. At 200 K the third region vanishes completely. In this case there exists only a one-diode model behavior. The parameters are determined according to the one-diode model. The six parameters, which are listed in Table 2, have been calculated from each measured curve. From 160 K onwards the variations of the

Table 1
Comparison of experimental and theoretical parameters

	I_{sc} (mA)	V_{oc}(mV)	FF (%)	η (%)
Measured	– 30.6	593.8	73.6	13.3
Calculated	– 30.6	592.4	72.1	13.1
Deviation from measurement value	0	– 0.23%	– 2%	– 1.5%

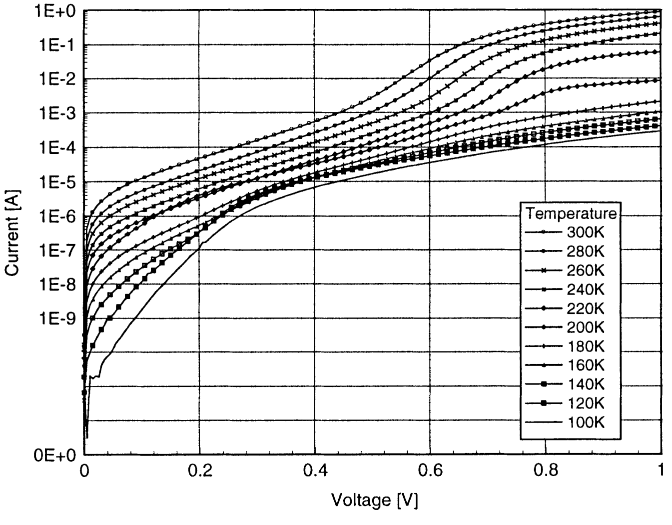

Fig. 4. Dark *IV*-curves for various temperatures.

Table 2
The parameters as obtained from dark *IV*-curves

T (K)	n_1	I_{01} (A)	n_2	I_{02} (A)	R_s (Ω)	R_{sh} (kΩ)
300	1.03	9.3E-12	3.13	4E-6	0.38	25
280	1.24	1.7E-11	3.25	1.6E-6	0.45	70
260	1.15	1.2E-13	3.75	1.1E-6	0.70	150
240	1.16	2.8E-15	4.00	5.6E-7	1.30	250
220	1.23	2.3E-16	4.46	3.6E-7	3.40	400
200	1.41	1.7E-16	(6)	7.3E-7	23.4	800
180			5.40	1.3E-7	100	1E + 3
160			5.20	3.5E-8	300	1E + 9

parameters are very little, so that in this case, the measured curves have only been analyzed and evaluated as far as 160 K. With the help of these parameters the dark *IV*-curves have been calculated and compared to the experimentally calculated *IV*-curves. Figs. 5 and 6 illustrates the comparison of the curves for 260 K (according to

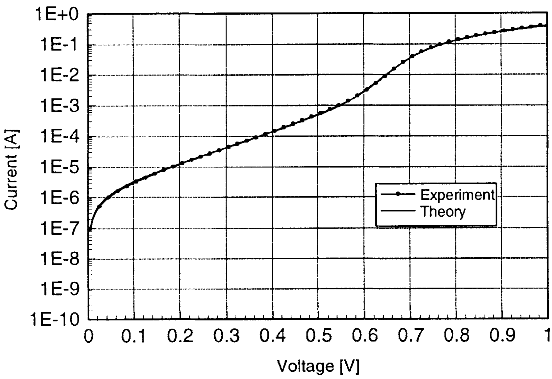

Fig. 5. Comparision of experimental and theoretical dark *IV*-curves at 260 K with the two-diode model.

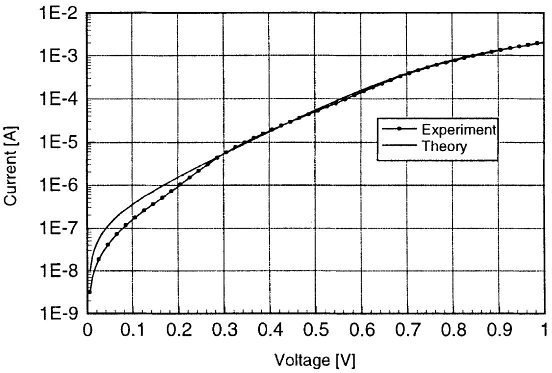

Fig. 6. Comparision of experimental and theoretical dark *IV*-curves at 160 K with one-diode model.

two-diode model) and 180 K (according to one-diode model). The good coincidence could also be established at all the other temperatures.

The ideality factor n_1 increases slightly with decreasing temperatures. However, the saturation current I_{01} decreases considerably, so that at low-temperatures diode 1 has no influence on the *IV*-curves. The ideality factor n_2 increases linearly with decreasing temperatures, whereas only a slight decrease in the saturation current I_{02} is observed. At low-temperatures diode 2 dominates.

5. Conclusion

We have investigated the dark *IV*-curve of an a-Si/c-Si heterojunction solar cell. The *IV*-curve could be described at room temperature with the help of the two-diode model. The parameters of the model have been determined and the *IV*-curve has been calculated from the measuring curve. The measured and the calculated curves have shown a very good coincidence. The ideality factors of the two diodes are as follows: $n_1 = 1.03$ and $n_2 = 3.13$. A voltage independence of the photocurrent has been confirmed with the validity of the superposition principle. During the investigation of the dark *IV*-curve of low temperatures the following has been found: up to 200 K the dark *IV*-curves could be described with the help of a two-diode model and under 200 K only with the help of a one-diode model. The ideality factor n_1 increases slightly and the ideality factor n_2 increases linearly with decreasing temperatures.

Acknowledgements

This work was supported by the AG Solar (NRW, Germany). The authors would like to thank K. Meusinger and B. Wdowiak for technical support.

References

[1] M.W.M. Van Cleef, Amorphous-Crystalline Silicon Heterostructures and Solar Cells, Ph.D. Thesis, University of Utrecht, 1998.

[2] D. Borchert et al., Sol. Energy Mater. Sol. Cells 49 (1997) 53.